

Supporting information

Transparent Conducting Oxide- and Pt-free Flexible Photo-Rechargeable Energy Storage System

Fayin Zhang, Weifeng Li, Zijie Xu, Meidan Ye, Wenxi Guo*^a, Hongyao Xu, Xiang-yang Liu

1. Experimental section

Materials. All chemicals were analytical grade and used as received. Ethanol, acetone, sulfuric acid, ammonium fluoride, isopropyl alcohol, diethanolamine, ammonium persulfate, aniline were purchased from Alfa Aesar. Cellulose acetate membrane was purchased from Shanghai Jinsui Bio-technology Co., LTD. Carbon Cloth was purchased from Beijing Huaxia New Technology Co., LTD. Ti foil was purchased from Shenzhen Suling Metal Materials Co., LTD.

Material preparation. TiO₂ nanotube arrays (TNARs) on the Ti foil: The TNARs were prepared by electrochemically anodizing method in ethylene glycol solution containing 0.3wt% of NH₄F and 2vol% of deionized water. Before anodization, the Ti foil was ultrasonically cleaned in acetone, deionized water and ethanol continuously in 15 minutes separately and then dried in air. The resulting Ti foil was anodized with two steps as reported in previous literature¹. The resulting anodized TNARs on both sides presents a layer with mesopores on the top of Ti foil. Subsequently, the TNARs was annealed at 450°C for 30 minutes in air to form anatase crystal structure with a high purity. Then the Ti foil was immersed in an aqueous solution of TiCl₄ at 70°C for 30 minutes, followed by annealing at 450°C for 30 minutes.

Assembly of dye-sensitized solar cell. For the dye-sensitized solar cell (DSSC), the photo-anode of the DSSC based on the TNARs was sensitized by a 0.3 mM cisbis(isothiocyanato)bis(2,2'-bipyridyl-4,4'-dicarboxylato) - ruthenium(II)bis-tetrabutylammonium dye (N-719 as received from Solaronix) solution in dry ethanol for 24 h. The transparent and highly conductive counter electrode (CE) was prepared by immersing the flexible Cu meshes, which was obtained by photo-lithography, (provided by Xiamen G-CVD Graphene Technology Co., Ltd.) into the saturated sulfur solution at 70°C for 12 hours. The dye-adsorbed TNARs electrode and the copper sulfide CE were assembled into a sealed sandwich-type cell using a liquid electrolyte including 0.5 M LiI, 50 mM I₂, and 0.5 M 4-

terbutylpyridine in 3-methoxypropionitrile.

Assembly of supercapacitor. The SC part on the other side of the Ti foil was made up of three components: anode, separator membrane, cathode. The anode was oriented TNARs that are directly grown on the other side of Ti foil. The surface of the TNARs was deposited by a layer of polyaniline through in-situ polymerization². An oxidized Ti foil was put into 1 M HCl, and 0.816 g aniline was added into the suspension solution and stirred for another 0.5 h before the temperature was then decreased to 0°C. 0.2 g APS was then added and the mixture was kept stirring at 0 °C for 24 h to achieve full polymerization. The cellulose acetate membrane was used as the separator between the cathode and anode. The cathode was an excellent conductive carbon cloth that was composited by polyaniline through electrochemical deposition using the constant potential method with 0.85 V for 1000s. Before placing the anode on the cathode, the supercapacitor was filled with PVA/H₃PO₃ gel electrolyte. Gel-type electrolyte was first prepared. 4 g of PVA was added into 40 mL of 1 M phosphoric acid, and the mixed solution was kept stirring at 90 °C for 1 h.

Characterization. A four-point probe (RTS-8) was used to measure the films' Rs. The light transmittances of all the TCEs were measured by UV-vis spectroscopy (Shimadzu UV-3600). The phase identification of the CuS NS sputtered CuS film electrodes was measured by X-ray diffraction (XRD) using a PANalytical X'Pert PRO diffractometer. The morphology and structure of the prepared materials were examined by scanning electron microscopy (SEM, Hitachi SU-70) and transmission electron microscopy (TEM, JEM 2100), respectively. For electrochemical properties was measured by using a CHI660E electrochemical workstation. The EIS was carried out on the symmetric cells to measure charge transfer resistance (R_{ct}) using a CHI 660E electrochemical workstation under a frequency range from 100 kHz to 0.1 Hz and the corresponding ac amplitude was 10 mV. The equivalent circuit models were used to analyse impedance spectra. The photovoltaic I-V measurement was performed under a solar simulator (500 W Model 91160, Newport) with an AM 1.5 spectrum to simulate a full-sun intensity (100 mW cm⁻²).

2. Figures

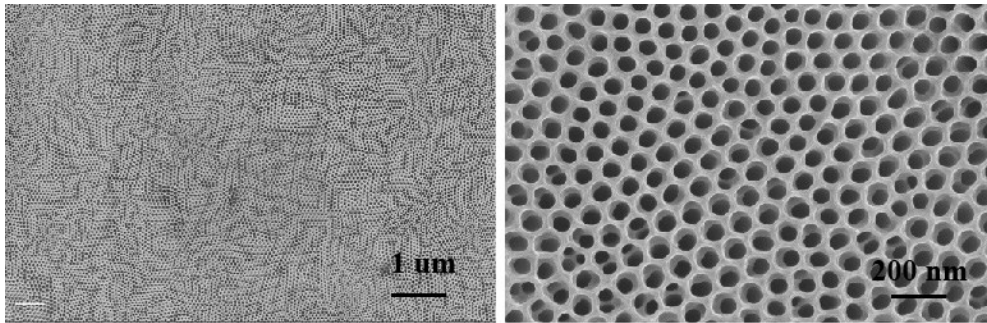


Fig. S1 The SEM image of the TiO₂ Nanotubes (TNARs). It follows from the SEM image that very uniformly aligned TNARs with diameters ~120 nm on the top surface after a two-step anodization.

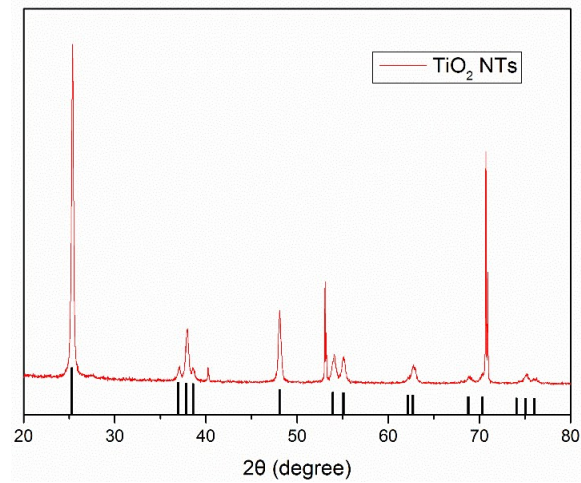


Fig. S2 XRD pattern of TNARs. The diffraction peaks located at 25.3°, 37.8°, 54.0° and 62.7° can be readily indexed to (101), (004), (105) and (204) of anatase TiO₂ phase, according to the Joint Committee on Powder Diffraction Standards (JCPDS card no. 21-1272).

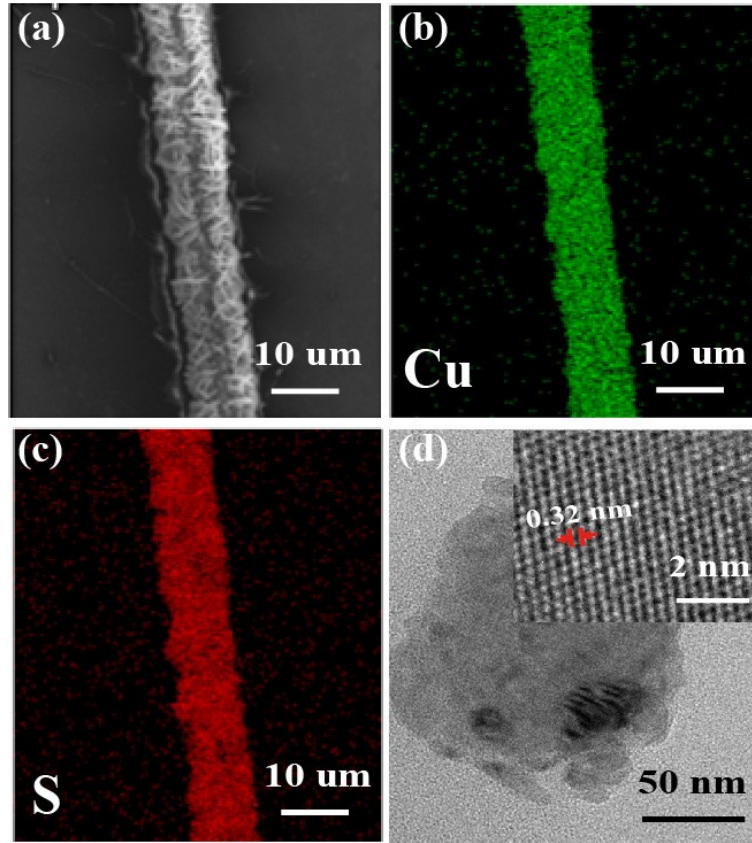


Fig. S3 (a-c) The elemental mapping image of S and Cu element XRD pattern of TNARs. The components of S and Cu are uniformly distributed in the CuS networks. (d) The TEM of the CuS nanosheet. The lattice spacing of 0.32 nm as marked in the inset matches with the lattice spacing of (101) planes for the hexagonal CuS phase, indicating that the CuS nanosheet grows along the [101] crystallographic direction.

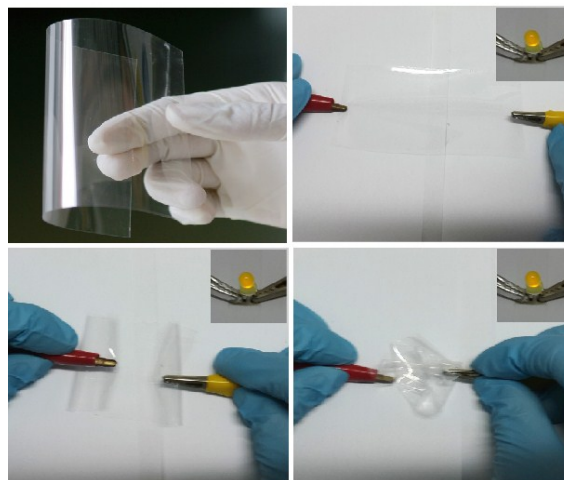


Fig. S4 The CuS network counter electrode was keep excellent electrical conductivity after bended and twisted.

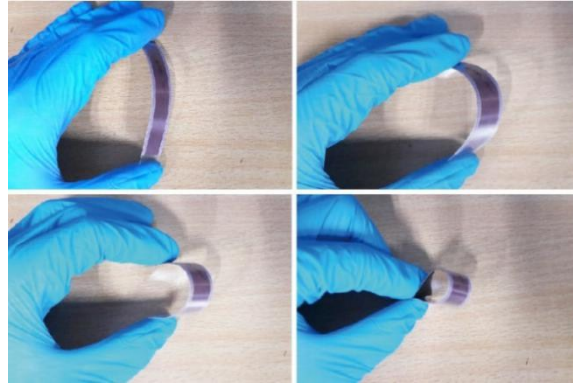


Fig. S5 The single dye-sensitized solar cell was bended at different angles.



Fig. S6 The photograph of single dye-sensitized solar cell.

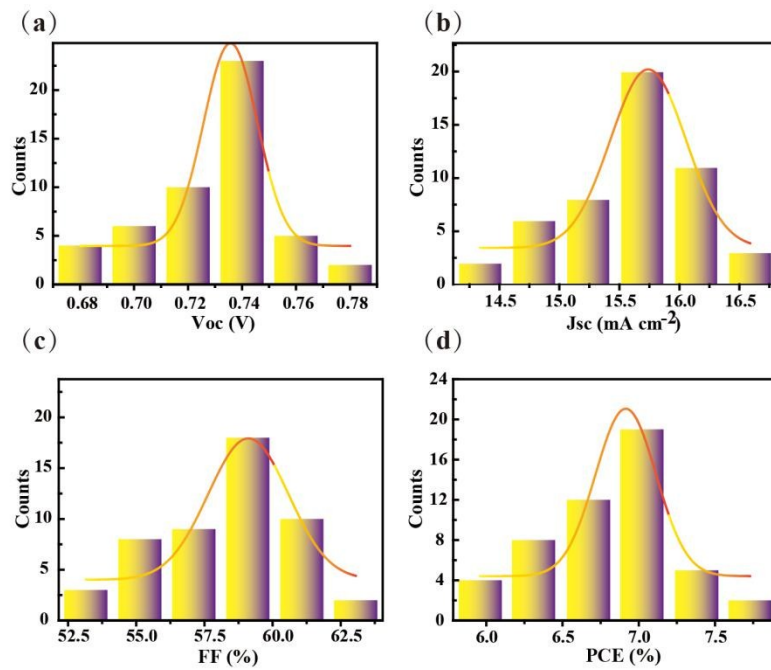


Fig. S7 The statistic of key parameters of randomly selected DSSCs. (a) V_{oc} , (b) J_{sc} , (c) FF and (d) PCE.

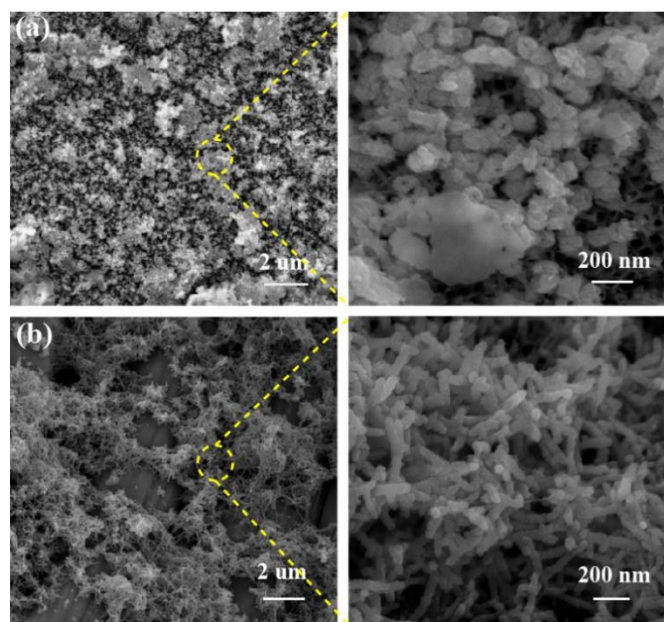


Fig. S8 (a) The SEM images of the TNARs-PANI composite electrode. A layer of granular PANI deposited on the top of TNARs. It is obvious that the PANI layer is deposited on the top surface of TNARs and the inset image reveals that the PANI was granulated with diameters of ~ 100 nm. (b) The SEM images of the CC-PANI composite electrode. Dense PANI nanorods are randomly deposited on CC and these nanorods are intertwined with each other to form the mesh structure, which is beneficial to increase the electrode specific surface area and promote transport channels for ions.

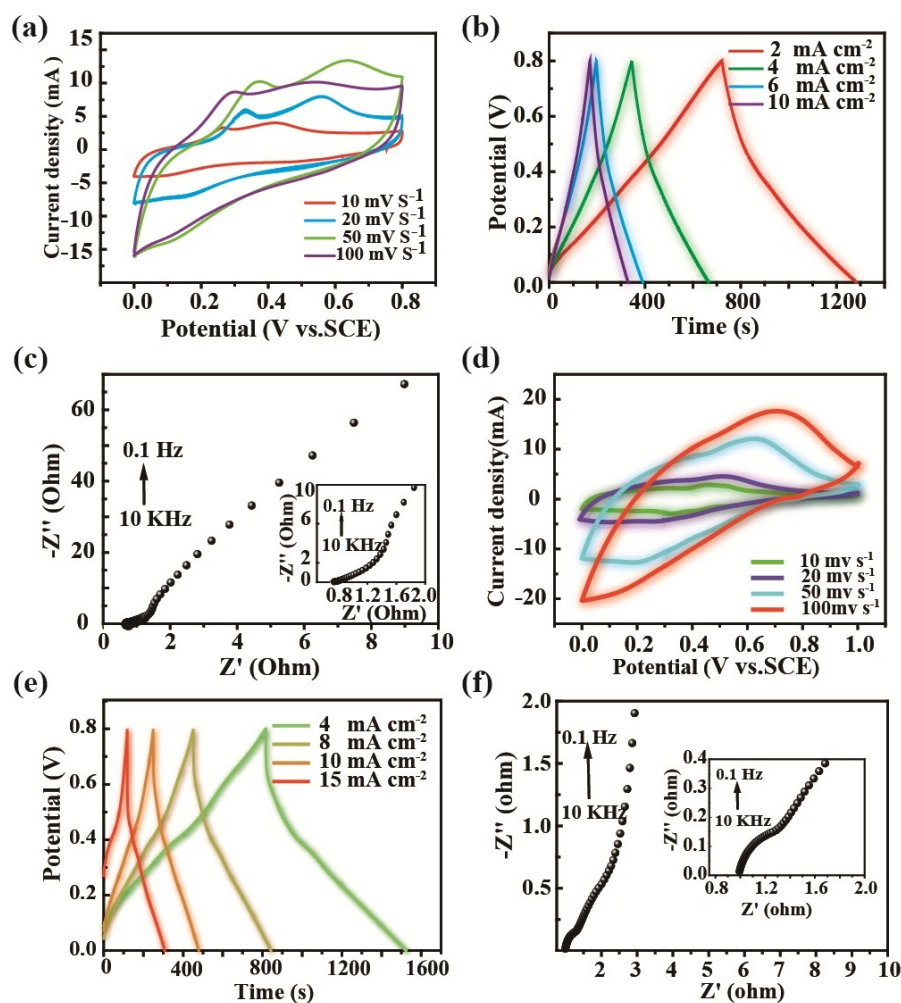


Fig. S9 (a) The CV curves of the TNARs-PANI electrode at different scan rates. CV curve of TNARs-PANI electrode displays a larger area compared with that of the pristine TNARs, which the electro-activity of the TNARs layer is very low in the anodic region (**Fig. S10**). For TNARs-PANI electrode, it has an obvious increase in the positive potential which may be caused by the recombination with PANI (b) GCD curves at different current densities of the TNARs-PANI electrode. According to the calculation, the maximum value of specific capacitance is 1.68 F cm^{-2} at a current density of 2 mA cm^{-2} . In addition, the specific capacitance still remains at 0.74 F cm^{-2} at a current density of 10 mA cm^{-2} , indicating high rate capability at high current density. (c) Nyquist plot of the TNARs-PANI electrode. According to the equivalent circuit, the solution resistance (R_s) and charge transportation resistance (R_{ct}) was obtained are $7.6 \Omega \text{ cm}^{-2}$ and $50.6 \Omega \text{ cm}^{-2}$, respectively, revealing that the TNARs-PANI electrode has a low diffusion resistance for ions transportation in the electrolyte low barrier in the faradaic reaction at the electrolyte/electrode interface respectively. (d) The CV curves of the CC-PANI electrode at different scan rates. The area of the CV curves increases with the scan rates, and the curves' shape reveals mainly faradic pseudo-capacitance. Since the CC itself is somewhat active as an electrode material for supercapacitors, the typical redox and reduction peaks for PANI is not observable in the CV curves. (e) GCD curves of the CC-PANI electrode at different current densities. The CC-PANI composite electrode has a maximum specific capacitance of 3.3 F cm^{-2} at a current density of 4 mA cm^{-2} . Simultaneously, the specific capacitance remains 2.26 F cm^{-2} at a current density

of 15 mA cm^{-2} which indicates excellent rate performance for CC-PANI composite electrode at high scan current density. (f) Nyquist plot of CC-PANI electrode. It was demonstrated the values of R_s and R_{ct} as low as $4.8 \Omega \text{ cm}^{-2}$ and $39.5 \Omega \text{ cm}^{-2}$, respectively.

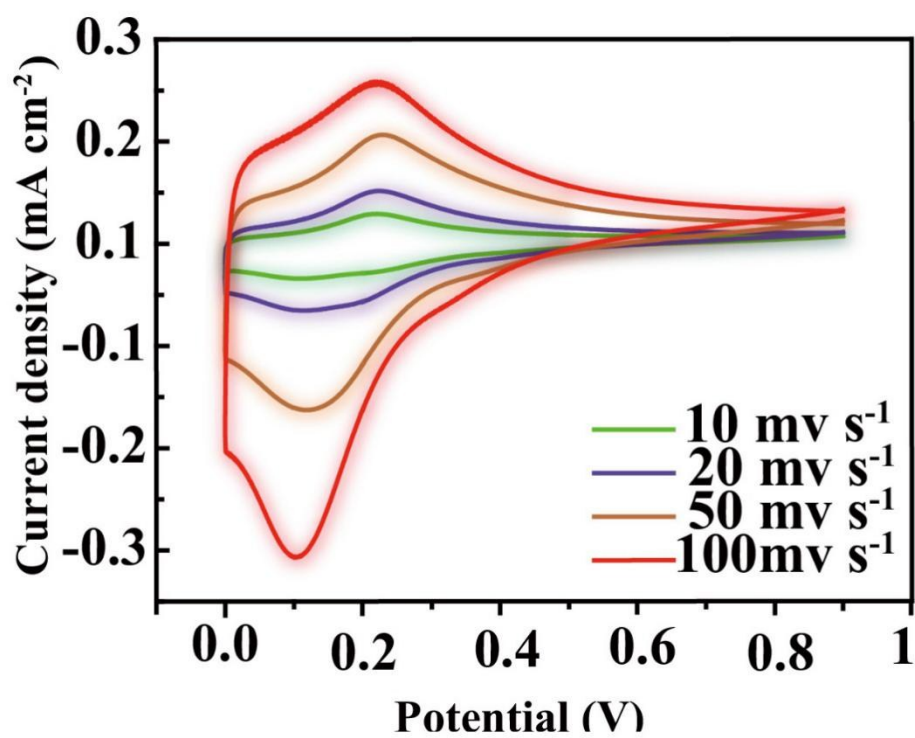


Fig. S10 CV curves of the pure TNARs electrode at different scan rates.

References

1. M. D. Ye, X. K. Xin, C. J. Lin, Z. Q. Lin, *Nano Lett*, 2011, **11**, 3214.
2. Y. Liu, Y. Ma, S. Y. Guang, F. Y. Ke, H. Y. Xu, *Carbon.*, 2015, **83**, 79.